Journal of Neonatal Surgery
ISSN(Online): 2226-0439
Vol. 14, Issue 18s (2025)
https://www.jneonatalsurg.com

OPEN ACCESS

Application of image processing in determination of erosion area in vacuum contacts

Hariom Patidar[1], Dr. Sunil Kushwaha[2]

[1]Research Scholar, Department of Computer Science and Engineering, Medi-Caps University, Indore, Madhya Pradesh, India, hariom.patidar@medicaps.ac.in
[2]Associate Professor, Department of Computer Science and Engineering, Medi-Caps University, Indore, Madhya Pradesh, India, sunil.kushwaha@medicaps.ac.in

Cite this paper as: Hariom Patidar, Dr. Sunil Kushwaha, et.al (2025) Application of image processing in determination of erosion area in vacuum contacts. *Journal of Neonatal Surgery*, 14 (18s), 286-292.

ABSTRACT
The efficacy and durability of vacuum switches are significantly affected by contact surface erosion during arc interruption. Nevertheless, the quantitative study of ablation regions remains inadequately investigated. This paper presents a technique based on image processing to assess the surface ablation area of vacuum interrupter contacts using four color models: RGB, HSV, HSL, and HSI. Employing LabVIEW tools, pictures of contact surfaces after arcing were analyzed using threshold segmentation, filtering, and enhancement methods to locate and quantify ablation zones. Experimental findings demonstrate that the RGB system ensures steady pixel distribution, but the HSV, HSL, and HSI models provide enhanced detail and less vulnerability to noise. Post-processing using Gaussian filtering and Laplacian improvement diminished the mean assessment error to around 2.45%, hence affirming the method's accuracy. This method establishes a dependable basis for measuring surface wear in vacuum switches and refining their design to extend service life.

Keywords: Vacuum interrupter, contact ablation, image processing, color models

1. INTRODUCTION

Vacuum switches use a vacuum environment as a medium and are extensively utilized in aircraft and other medium to low voltage power systems owing to its benefits, including a small construction, ease of maintenance, lack of pollution, and robust breaking capability [1–3]. The vacuum arc extinguishing chamber is the primary element of vacuum switches, and failures in interruption caused by the structure and substance of the contacts leading to arc reignition are among the obstacles that impede the fast advancement of vacuum switches [4–6]. Currently, research on contacts is mostly categorized into two aspects: Examine and assess the impact of contacts, including their structures and materials, on the evolution of various physical phenomena such as temperature, electric, and magnetic fields in the vacuum arc extinguishing chamber, offering guidance for regulating arc shape and enhancing the interrupting capacity of vacuum switches [7,8]. Among them, scientists like Li Can [9] have developed a system for the direct monitoring of the contact temperature inside the arc extinguishing chamber. Initially, a contact model was used to simulate and study the electromagnetic temperature multiphysics coupling impact inside the arc extinguishing chamber. Subsequently, partial least squares regression was used to compute the ambient temperature, upper contact arm temperature, and other variables to provide real-time monitoring of contact temperature. Researchers like Dong Huajun [10] employed finite element analysis to perform bidirectional coupling simulation on the temperature field of the arc extinguishing chamber, determining the impact of structural factors such as contact diameter, contact plate thickness, cup holder thickness, and contact plate slot length on the temperature field. Researchers, including Yang Jinwang [11], investigated the magnetic field properties of cup-shaped longitudinal magnetic contacts under conditions of significant opening distance, concluding that augmenting the slot rotation angle can substantially improve the longitudinal magnetic field between contact systems. Investigate and evaluate the physical processes occurring on the surfaces of contact materials, including ablation, fatigue life, and plastic deformation, to enhance the design of vacuum interrupters and extend their operational lifespan [12,13]. Researchers, including Zhang Zaiqin [14], performed anode melting studies on four materials: W, Mo, Cr, and Fe, during the high current vacuum interruption procedure with a stationary Cu cathode. The maximum temperatures of the four materials and their respective melting point discrepancies were recorded. Simultaneously, the researcher examined the surface ablation process of anode materials and synthesized the impact of contact materials on anode ablation [15]. Researchers, including Wang Lijun [16], synthesized and evaluated the two-dimensional and three-dimensional simulation outcomes of cathode spots on the ablation morphology of contact materials, while addressing the limitations of diverse experimental and simulation investigations. Researchers Dong Huajun and Li Dongheng have investigated the fatigue life of contacts. Dynamic simulation investigation revealed that the convex support plate enhances the rational distribution of stress structures among contacts [17].

The study indicates that research on the contacts, materials, structures, and associated aspects of vacuum arc extinguishing chambers constitutes a significant direction in this subject. Nevertheless, no academics have conducted an evaluation or study of the ablation area of the contacts, resulting in an absence of quantitative analytical data in this domain. The irregular distribution or excessive ablation of the contact material's surface may lead to heightened roughness, and in extreme instances, aberrant protrusions and depressions may develop on the contact surface. Irregular protrusions and indentations on the contact surface may disrupt the normal emission of electrons, leading to the formation of cathodic spots necessary for completing the breaking job, while bigger protrusions may impede the appropriate closure of moving and stationary contacts. The erosion and cumulative wear on the contact surface resulting from a single breaking current or multiple opening and closing actions of the vacuum switch will influence the development of various physical fields within the arc extinguishing chamber, consequently impacting the contact's service life. Consequently, the quantitative assessment of the surface ablation phenomena in contacts is crucial for enhancing the overall efficacy of vacuum switches. Image processing technology is characterized by non-contact capabilities and great precision, and has been used in the study of vacuum switches. Scholars, including Dong Huajun [18], used image processing technologies to assess the movement velocity of the contacts. Zhang Zuofan [19] used graphic processing technologies to display the flow and temperature fields of vacuum arcs. Researchers like Li Gangsong [20] examined the arc in DC breaking and used image processing technologies to assess motion features and investigate picture parameterization. The integration of color science theory with image processing technology has been conducted for scientific research purposes [21–23]. Liu Yucheng [24] discovered that color-based image processing techniques may successfully address the issue of color offset in gathered data, hence enhancing the stability of test findings. Hu Yu [25] and other researchers conducted morphological analyses of the visible light wavelength images of electric halos and discharges, and undertook first investigations into color characteristics.

This article presents a technique for the quantitative evaluation of the surface ablation area of vacuum switch contacts. This approach utilizes chromaticity theory and image processing tools. The region is assessed using four color models: RGB, HSV, HSL, and HSI. The assessment accuracy of each color system is then tested using sample analysis technologies. The assessment plan for the contact ablation area is established by integrating the attributes of the contact ablation picture with the operational features of each color system. Ultimately, image processing technology is used to enhance assessment precision.

2. EVALUATION PRINCIPLE

This research presents a technique to evaluate the surface ablation area of vacuum interrupter contacts. This approach employs image processing methods to assess the region across four color dimensions: RGB, HSV, HSL, and HSI. In the RGB color model, each pixel is represented by three primary colors: red, green, and blue. The HSI, HSV, and HSL color systems may all be derived from the RGB color system. HSI refers to the hue saturation intensity color system, HSL denotes the hue saturation lightness color system, while HSV signifies the hue saturation value color system [26,27].

The RGB color model consists of three primary color components: red (R), green (G), and blue (B). The hue of each pixel is ascertainable from the intensity levels of these three components. This model is extensively used in image processing for color analysis. The HSV color model consists of three components: hue (H), saturation (S), and brightness (V). In the HSV model, hue (H) denotes the color type, saturation (S) indicates color purity, and brightness (V) reflects color luminance, facilitating a more natural description of color properties. The HSL color model resembles the HSV model. The distinction lies in the brightness (L) component of HSL, which defines the extent of lightness and darkness of a color, making it more appropriate for articulating variations in illumination and surface luminance. The HSI color model resembles the HSV model; however, it characterizes brightness via intensity (i) and employs saturation (s) and hue (H) to denote color purity and type. Following the disintegration of the vacuum arc extinguishing chamber post-arc drawing experiment, this investigation was conducted in accordance with the procedure shown in Fig. 1. During the experiment, contact photos exhibiting burn marks were loaded into the LabVIEW virtual instrument platform. Initially, edge enhancement technology and threshold segmentation methods were used to delineate the contact region and the burn area of the contact surface. The Vision Builder development software was then used to conduct pixel statistics on the segmented contact area and the contact surface burn area.

3. ANALYSIS OF IMAGE FEATURES OF CONTACT BURNOUT

This experiment utilizes un-eroded photos and contacts, with a discount applied after 200 cuts, indicating that the images of erosion serve as the study subject. The ablation region on the surface resembles a circle or an oval. The distribution of the unclear regions lacks discernible regularity, howevJer the degree of ablation in the center of the contact is moderate. The ablation increases with the radius. Furthermore, as seen in Fig. 1, the extent of ablation on the left side of the tentacles exceeds that on the right side. The reason of this occurrence requires more study and analysis. The contact photos and erosion images are imported into LabView software for statistical analysis of pixel value distribution. This experiment is fundamentally concerned with the distribution of pixel values among the four-color systems: RGB, HSV, HSL, and HSI. In the RGB color scheme, the pixel count corresponds to the maximum value of R, G, and B across the three components, totaling 61,632 pixels at the specified pixel value. The ultimate peak of B component occurs at a pixel value of 120, corresponding to 64,522 pixels. In the HSV, HSL, and HSI three-color systems, the pixel counts of each component are separately distributed, exhibit little overlap, and demonstrate a broad range of pixels. The H component has a multi-peak

structure throughout the three systems. The pixel distribution of S components across the three systems is mostly concentrated within the pixel value range of around 0–50. The three components of I, V, and L are fundamentally same throughout the three systems, occurring between the ranges of around 75-100 and 200-225. The maximum quantity of pixels for each pixel value of i, V, and L does not exceed 20,000.

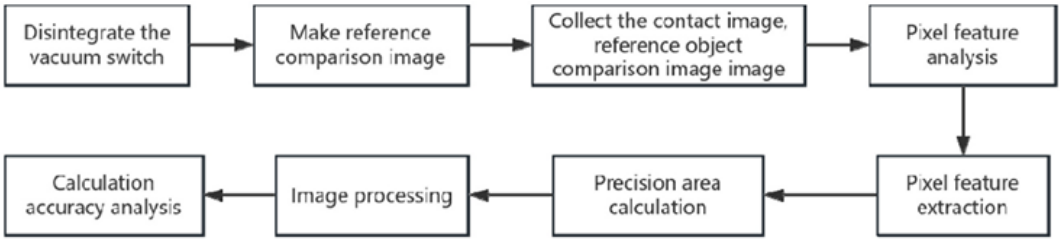

Fig. 1. Experimental flow chart

The pixel range value for the third area is between 171 and 225, and the trend of the three components exhibits a secondary peak. During the second peak stage, the pixel counts for the R, G, and B components each reached around 79,000 at a pixel value of around 200, thereafter declining to roughly 1,000 at a pixel value of approximately 220. In the fourth stage, the pixel range spans from 226 to 255, with the pixel count for the three components consistently remaining around 1000. The modifications in the five elements of H, S, I, V, and L The pattern in pixel value variations across the three systems is fundamentally consistent with the alterations seen in the contact photographs; however, the quantity of pixels corresponding to each weight value will diminish this tendency. The quantity of pixel values for each pixel value of i, V, and L is diminished, with the maximum value not surpassing 10,000. The pixel information comparison of the picture before to and after to the touch is discernible inside the RGB system: In the RGB system, when the contact surface is occluded, the red (R) component may intensify, particularly with rising temperatures, resulting in increased redness in the ablation region. The green and blue (G and B) components may diminish, indicating a darkening or obscurity of the surface hue. In the HSV system, the ablation zone may undergo hue alterations, with the contact surface transitioning from metallic to red or gray, indicative of variations in surface temperature and material composition. The saturation (s) will decrease, signifying that the hue of the obscured region is no longer pristine; the brightness (V) will diminish, showing a reduction in the luminosity of the ablation area. Analogous to HSV in the HSL system, the luminance (L) in HSL emphasizes the variations in lightness and darkness of the color. The ablation zone may exhibit a darker region, indicating an increase in the surface roughness of the contaminated area of the contact material.
In the HSI system, the intensity (i) in HSI fluctuates with the advancement of the ablation, and the decrease in intensity signifies a less capacity to reflect light from the surface of the contact material.
The pixel distribution of the contact picture in the RGB system is more consistent, and the three components are better harmonized. In the three-color systems of HSV, HSL, and HSI, the pixel counts of each component in pictures exhibit more independence, therefore more accurately representing the detailed information of pixels. The HSI three-color systems have robust anti-interference capabilities in each component.

4. EVALUATION OF THE ABLATION ZONE BY CONTACT IMAGING

4.1. Evaluation of Contact Crater Area

The precise procedure for assessing the area of contact melting pits is as follows: (1) Background segmentation is executed on the ablated contact picture, and standardized square test specimens with a side length of 1–10 mm are fabricated (rounded); (2) Acquire and transmit contact ablation images alongside comparison images, with selected acquisition results shown in Fig. 2; (3) Threshold segmentation is executed utilizing the four color systems: RGB, HSI, HSL, and HSV, to identify the contact area, ablation area, and specimen area; (4) A combination of filtering and integration functions is employed to eradicate image noise and augment edge information across diverse regions; (5) Pixel statistics are utilized to assess the pixel count in various regions.

4.2. Evaluation and error analysis of ablation area in RGB color system

In the RGB color system, the color characteristics of each pixel in a color image can be represented by three primary colors and quantity values.

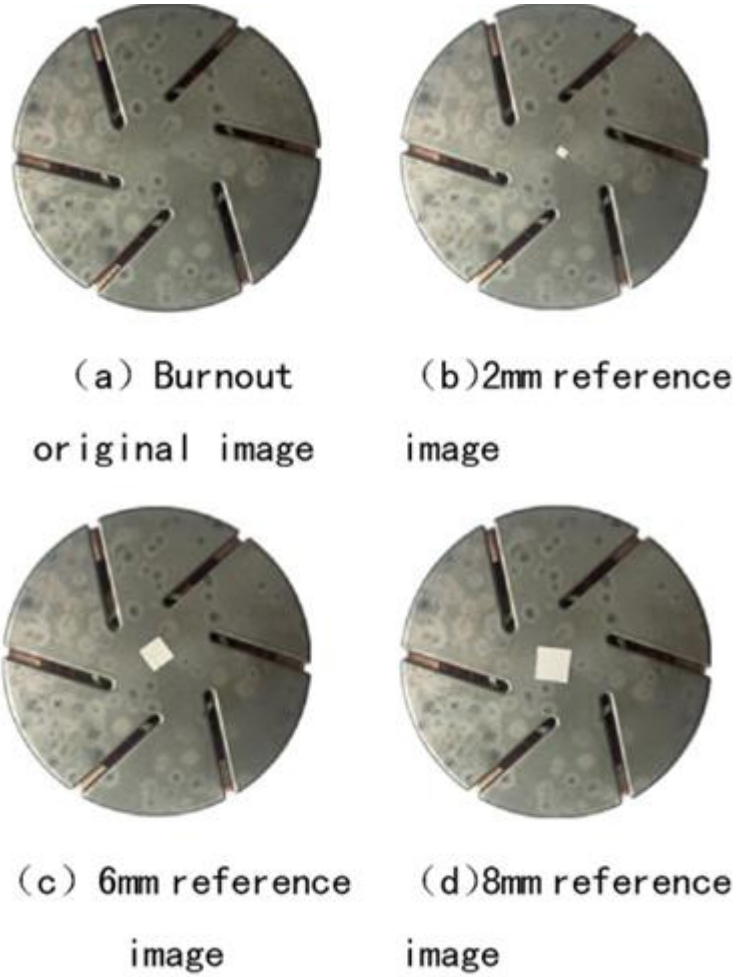

Fig. 2. Contact erosion and comparative images

The contact ablation picture has several pixels, with the chromaticity attributes of each pixel dictated by the varying component values of the R, G, and B primary colors. Experimental statistical analysis has shown that the dimensions of the ablation region and specimen area in the contact ablation picture correlate closely with the magnitude of the R component in the RGB ratio [28]. A portion of the statistical findings is shown in Table 1. When the areas are same, the standard deviation of the R component is minimized. As the area varies, an increase in the ablation area and specimen area correlates with a reduction in the standard deviation of the R component value, resulting in more stable statistical data [29]. Consequently, this research employs the technique of extracting the R component to attain the impact of picture grayscale and advance to the subsequent operational phase. Upon finalizing the grayscale of the contact image and the comparison picture, threshold segmentation is performed for the contact area, ablation region, and test area. The Vision Builder processing package on the LabView platform specifies a target picture amplification value of 100, applicable just to pixel feature statistics inside the designated region. Figure 3 presents a pixel information statistics picture with a trial area with a side length of 10 mm.

The pixel range value of the contact area is established as (180, 220), the area value of the ablation area pixels is between (70, 170), and the pixel area of the test film is between (220, 240). The evaluation findings demonstrate that, when assessing the overall size of the ablation zone using this approach, an increase in specimen area correlates with a heightened assessment error. When the side length of the test specimen area is 10 mm, the evaluation error attains 5.23%, perhaps attributable to picture noise. In threshold segmentation, an increase in the test piece's area correlates with a broader pixel range and a higher pixel count, leading to diminished accuracy in the assessment outcomes. To enhance assessment accuracy, the introduction of image processing methods is proposed to mitigate the effects of picture noise on the findings.

Table 1 Standard deviation of RGB values for different components

Standard deviation of each component	4 mm^2	9 mm^2	16 mm^2	25 mm^2
R	50.01	49.97	49.84	49.62
G	50.88	52.25	50.77	51.40
B	52.91	53.36	52.94	53.43

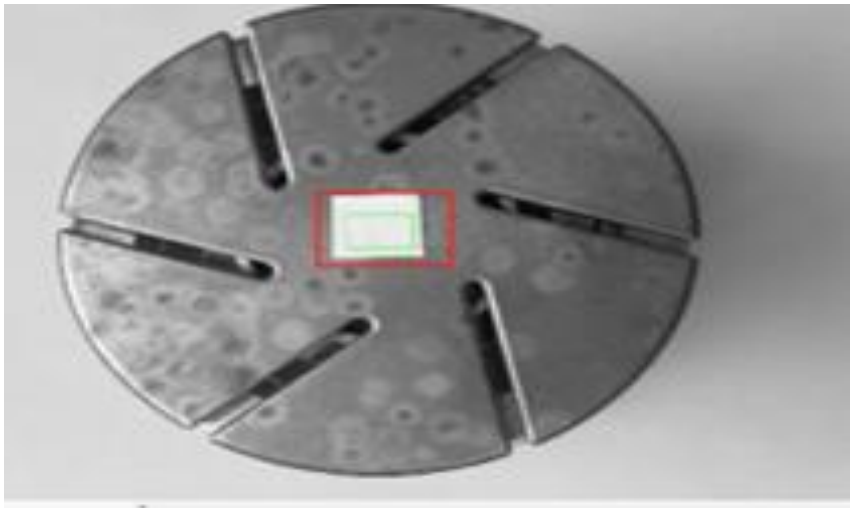

Fig. 3. Reference object threshold extraction

The HSI, HSV, and HSL color models may execute picture grayscale and threshold segmentation at the I, V, and L components correspondingly. The pixel ranges for the contact area, ablation area, and specimen area within the aforementioned three-color systems using LabVIEW pixel statistics. The total area of contact ablation was assessed in the RGB, HSV, HSL, and HSI color systems as 149.78 mm², 152.24 mm², 131.97 mm², and 167.6 mm², respectively. The greatest ablation area of the melt pit in each color scheme was under 20 mm².

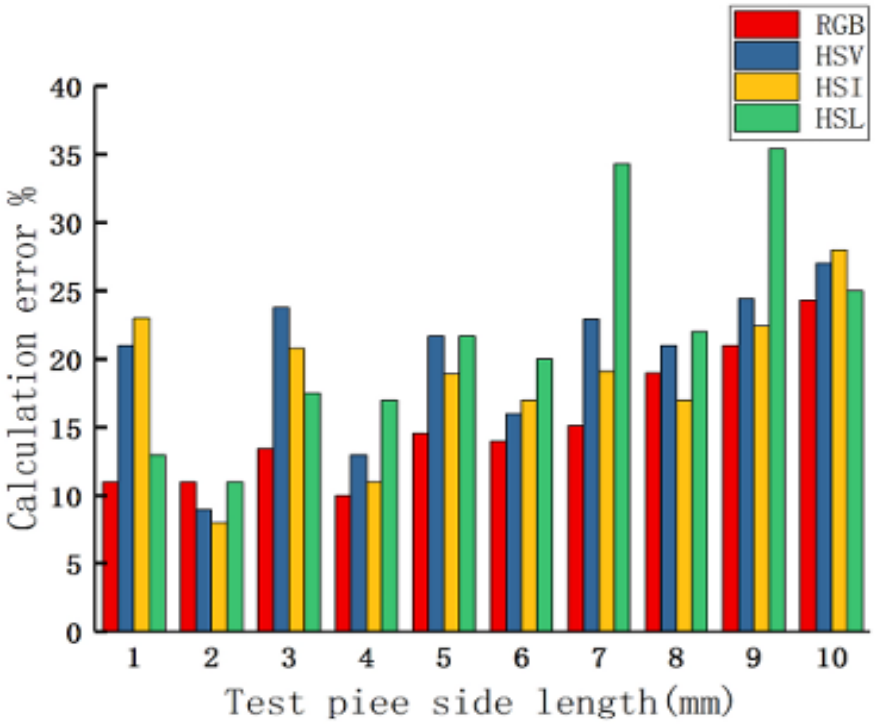

Fig. 4. Comparison of calculation errors

5. IMAGE PROCESSING AND ANALYSIS OF CALCULATION RESULTS

5.1. Image processing

This article employs four image denoising techniques from the Labview virtual instrument platform: low-pass filtering, Gaussian filtering, median filtering, and bilateral filtering, along with five image enhancement methods: Sobel, Laplacian, Prewitt, Roberts, and Difference, to enhance the precision of the calculation results. Among them, Prewitt, Roberts, and Differentiation, three image enhancement techniques, failed to adequately maintain the essential information of the picture throughout processing. Consequently, eight experimental protocols for image processing were first established. In the experiment, the filtering kernels for the four filtering functions were set to 3, while the convolution kernels for the Sobel and Laplacian convolutions were configured to 7. The experiment determined that using Gaussian filtering for denoising and the Laplacian convolution function for picture augmentation yielded the greatest computational accuracy. Subsequent to image processing, threshold segmentation is reapplied to ascertain that the pixel range value of the contact region is

(175–220), the pixel range value of the ablation area is (73–162), and the pixel range value of the reference area is (220–234).

5.2. Analysis of calculation results

Following the use of picture denoising and enhancement techniques inside the HSV color model, the assessment error of this approach was reduced. The cumulative ablation area of the contact ablation picture is 151.17 mm², with the peak ablation area recorded at 10.37 mm². In comparison to the pre-image processing findings, the mean evaluation error for each area interval is around 2.45%; while assessing the area range of 16 mm², the evaluation error may be maintained within 3%.

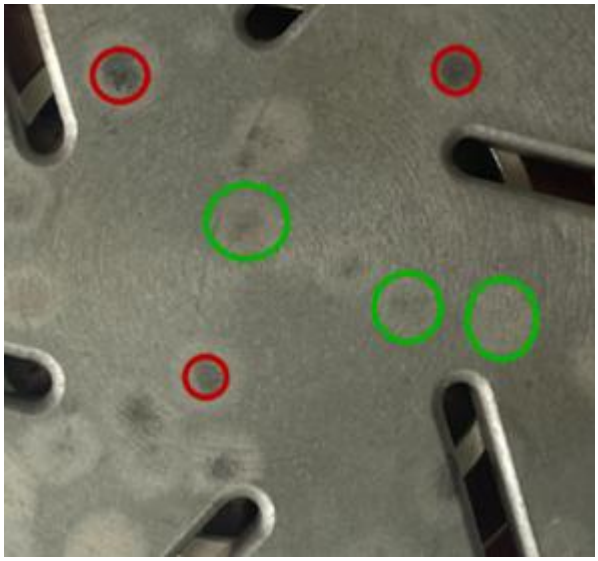

Fig. 5. Surface erosion

The experiment revealed many elements that influence the accuracy of this algorithm's calculations: The chosen contact surface for this experiment has a uniform distribution of six slots, designed to mitigate erosion and control the electric, magnetic, and thermal fields throughout the opening and closing phases. During pixel counting, some pixels in the slotted area were erroneously included in the ablation area, leading to a calculated result that exceeded the actual area. Figure 5 delineates the charred area on the contact surface into two distinct types. One category of red region exhibits a moderate level of erosion, characterized by a pixel range of around (101–151), whilst the other category of green area displays a more severe level of erosion, with a pixel range of approximately (70–170). The ablation area was calculated without individually accounting for the two kinds of areas, relying only on the average pixel range of regions with a greater degree of ablation as a threshold parameter for pixel statistics, leading to findings that were discordant with actual conditions.

6. CONCLUSION

TTis study introduces a methodical and precise approach for measuring the ablation area of vacuum switch contacts via image processing and chromaticity theory. The research compared four color models—RGB, HSV, HSL, and HSI—and concluded that although RGB provides uniform pixel distribution, the HSI model demonstrates superior anti-interference and more precise detail representation. The suggested image processing pipeline, including Gaussian filtering and Laplacian augmentation, substantially diminished noise and augmented the dependability of pixel-based area evaluations. Following augmentation, the mean error in ablation area computation decreased to 2.45%, with a maximum error of less than 3% for sections measuring 16 mm². This approach not only addresses the deficiencies in the quantitative evaluation of contact degradation but also enables future improvements in vacuum switch reliability, predictive maintenance, and design optimization.

REFERENCES

1. Huajun Dong, Peng Sun, Li Dongheng, Etc Calculation and structural optimization of the electric repulsion force of the 12-kV vacuum arc extinguishing chamber contact, High Volt. Eng. 48 (9) (2022) 3602–3611.
2. Dong Huajun, Cheng Jingzhou, Zhao Yijian, Etc Simulation analysis of transient characteristics during the breaking process of high current vacuum arc [J] Journal of Electrical Machinery and Control, 1-9.
3. Li Hongxu, Bin Xiang, Etc the method of full current breaking coordination between superconducting current limiters and mechanical DC circuit breakers, High Voltage Technology 48 (11) (2022) 4497–4505.
4. Zhao Shutao, Huang Weijie, Liu Huilan, Yang Jiarui, Liu Yunpeng A review of research on contact erosion and electrical life assessment of high-voltage circuit breakers [J] High Voltage Technology, 1-148.
5. Gan Zhizheng, Yu Zhanqing, Qu Lu, Etc Natural commutation type DC circuit breaker based on vacuum

switch and gas switch series connection [J] Proceedings of the CSEE, 1-10.
6. Yifei Wu, Jiahao Guo, Fei Yang, Jianying Zhong, Zhang Youpeng Analysis of motion characteristics of high-speed repulsive mechanism for DC fast switch, J] High Voltage Technology 44 (5) (2018) 1641–1650.
7. Sun Wanjie, Shi Yuxin, Ding Jianxiang, Etc New Ti_ (2) Preparation of Cd reinforced silver based electrical contact materials and their arc erosion resistance characteristics [J] Material Introduction, 1-18.
8. Huajun Dong, Kang Kai, Zang Kan, Etc Experimental study on arc flow field of vacuum switch based on PIV technology, Chinese Journal of Vacuum Science and Technology 34 (6) (2014) 590–592.
9. Can Li, Xian Daily, Cui Yong, Hu Yuyao, Sun Fengrui Indirect calculation of contact temperature in the arc extinguishing chamber of KYN series 12 kV switchgear vacuum circuit breaker, High Voltage Technology 49 (10) (2023) 4355–4363.
10. Huajun Dong, Chaoyang Wen, Linlin Liu, Etc Simulation of the influence of contact system structure on the temperature field of vacuum arc extinguishing chamber, J] Electric Machines and Control 27 (8) (2023) 164–172.
11. Jinwang Yang, Tao Tan, Shixin Xiu, et al., Magnetic field characteristics of cup-shaped longitudinal magnetic contact gap under large opening conditions [J], High Voltage Technology 49 (07) (2023) 3125–3133.
12. Huajun Dong, Peng Sun, Etc research on mechanical characteristics of vacuum circuit breaker rigid-flexible coupling system considering electric repulsion [J] electric machines and control 27 (3) (2023) 147–157.
13. Xinzhe Song, Minfu Liao, Etc Research on the triggering characteristics of vacuum switch triggered by three gap laser, Trans. China Electrotech. Soc. 38 (14) (2023) 3923–3929.
14. Zhang Zaiqin, Liu Zhiyuan, and Others Experimental and Simulation Research on Anode Melting Process in High Current Vacuum Arc [J] Transactions of China Electrotechnical Society, 1-11.
15. Zai Qin Zhang, Wang Chuang, Others Research progress on anode ablation process in high current vacuum arc, Vacuum Electronics Technology (5) (2023) 25–34.
16. Lijun Wang, Wang Cong, Etc Summary of experimental and modeling simulation studies on the ablation morphology of vacuum arc cathode spots, Vacuum Electronics Technology (5) (2023) 1–10+34.
17. Huajun Dong, Li Dongheng, Etc Research on fatigue life of 12kV vacuum arc extinguishing chamber contacts under closing impact, Trans. China Electrotech. Soc. 37 (15) (2022) 3981–3988.
18. Huajun Dong, Liting Ma, Li Jie, Etc Vacuum switch opening speed detection based on image processing technology, High Voltage Technology 46 (7) (2020) 2539–2544.
19. Zuofan Zhang, Visualization of Vacuum Arc Flow Field and Temperature Field Based on Image Processing Technology [D], Dalian Jiaotong University, 2023.
20. Li Lansong, Image Processing and Parameterization Research on DC Breaking Arc [D], Dalian University of Technology, 2019.
21. G.R. Jones, Plasma monitoring using chromatically processed optical fibre signals, Proc. 21th ICPIG P1–24 (1993).
22. G.R. Jones, et al., Chromatic modulation-based metrology, Pure and Applied Optics 2 (p87) (1993).
23. Ying Wang, et al., Chromaticity method for on-line monitoring of high voltage switches, High Volt. Appar. 3 (1996) p34–p38.
24. Yucheng Liu, Zhang Yingchao Image chromaticity segmentation based on white balance algorithm, J] Computer Engineering 38 (20) (2012).